IVYSPRING
INTERNATIONAL PUBLISHER

Theranostics

Research Paper

Cell-Specific Promoters Enable Lipid-Based Nanoparticles to Deliver Genes to Specific Cells of the Retina *In Vivo*

Yuhong Wang[1,4*], Ammaji Rajala[1,4*], Binrui Cao[5], Michelle Ranjo-Bishop[1,4], Martin-Paul Agbaga[1,4], Chuanbin Mao[5,6✉] and Raju V.S. Rajala [1,2,3,4✉]

1. Departments of Ophthalmology, University of Oklahoma Health Sciences Center;
2. Departments of Physiology, University of Oklahoma Health Sciences Center;
3. Departments of Cell Biology, University of Oklahoma Health Sciences Center;
4. Dean McGee Eye Institute, Oklahoma City, OK 73104, USA;
5. Department of Chemistry and Biochemistry, University of Oklahoma, Stephenson Life Science Research Center, Norman, OK 73019, USA;
6. School of Materials Science and Engineering, Zhejiang University, Hangzhou, Zhejiang 310027, China.

* Y.W. and A.R. equally contributed to this work.

✉ Corresponding authors: **Email:** raju-rajala@ouhsc.edu; cbmao@ou.edu.

Abstract

Non-viral vectors, such as lipid-based nanoparticles (liposome-protamine-DNA complex [LPD]), could be used to deliver a functional gene to the retina to correct visual function and treat blindness. However, one of the limitations of LPD is the lack of cell specificity, as the retina is composed of seven types of cells. If the same gene is expressed in multiple cell types or is absent from one desired cell type, LPD-mediated gene delivery to every cell may have off-target effects. To circumvent this problem, we have tested LPD-mediated gene delivery using various generalized, modified, and retinal cell-specific promoters. We achieved retinal pigment epithelium cell specificity with vitelliform macular dystrophy (VMD2), rod cell specificity with mouse rhodopsin, cone cell specificity with red/green opsin, and ganglion cell specificity with thymocyte antigen promoters. Here we show for the first time that cell-specific promoters enable lipid-based nanoparticles to deliver genes to specific cells of the retina *in vivo*. This work will inspire investigators in the field of lipid nanotechnology to couple cell-specific promoters to drive expression in a cell- and tissue-specific manner.

Key words: Lipid nanoparticles, Gene therapy, Retina, Retinal pigment epithelium, Ganglion cells, Cell-specific promoters.

Introduction

Lipids, with their hydrophilic and hydrophobic properties, provide a potent toolbox for nanotechnology [1]. They can be self-assembled into nano-films and other nano-structures, including micelles, reverse micelles, and liposomes [1]. Lipid-protamine-DNA (LPD) complexes have been characterized for *in vivo* gene delivery with reporter plasmid constructs [2;3]. Our laboratory has shown that cell targeting and cell-specific peptides (homing peptides) integrated into LPD can increase the efficiency of gene delivery into mammalian cells [4;5]. In 2014, we demonstrated for the first time that nanoparticle-assisted targeted delivery of eye-specific genes significantly improved the vision of blind mice *in vivo* [6].

One of the limitations of LPD is cell specificity [7]. However, in our earlier study, LPD-mediated gene delivery successfully restored visual function in mice that lacked this function, as the delivered gene was only expressed in one type of retinal cell [6]. If the

same gene is expressed in multiple cell types, LPD-mediated gene delivery may have off-target effects. The retina is composed of seven different kinds of neural cells. Therefore, there is a need for cell-specific delivery of LPD nanoparticles.

To demonstrate the significance and innovative nature of LPD in the retina, we first showed that cell-specific promoters enabled lipid-based nanoparticles to deliver genes to specific cells of the retina *in vivo*. In the present study, we achieved retinal pigment epithelium cell specificity with vitelliform macular dystrophy (VMD2), rod cell specificity with mouse rhodopsin, cone cell specificity with red/green opsin, and ganglion cell specificity with thymocyte antigen promoters (Fig. 1).
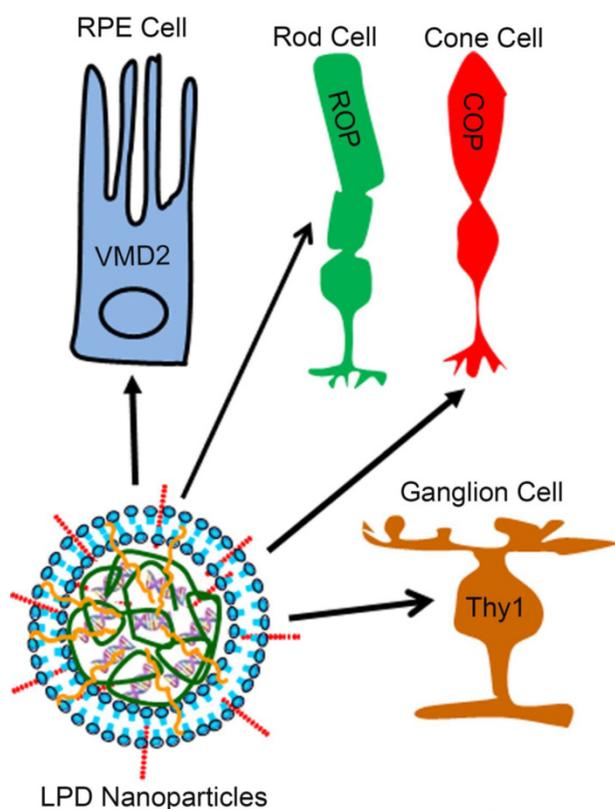
Figure 1. Retinal cell-specific delivery of genes. A liposome protamine/DNA lipoplex (LPD) integrated with a nuclear localization signal (NLS) peptide and transactivator of transcription (TAT) peptide was constructed for delivery of genes to retinal pigment epithelium (RPE) cells, rod cells, cone cells, and ganglion cells of the retina using cell-specific promoters. We achieved RPE cell specificity with vitelliform macular dystrophy (VMD2, 583 bp), rod cell specificity with mouse rhodopsin (225 bp), cone cell specificity with human red/green opsin (2100 bp), and ganglion cell specificity with thymocyte antigen (*Thy1.2*, 6500 bp) promoters.

Materials and Methods

Materials

The lipids, 1,2-dioleoyl-3-trimethylammonium-propane (chloride salt; DOTAP), 1,2-dioleoyl-*sn*-glycero-3-phosphoethanolamine (DOPE), and cholesterol were obtained from Avanti Polar Lipids,

Inc. (Alabaster, Alabama). The nuclear localization peptide (NLS, DKKKRKVDKKKRKVDKKKRKV) was procured from United Biosystems, Inc. (Herndon, Virginia). The TAT-peptide (YGRKKRRQRRR) was synthesized by Biosynthesis, Inc. (Lewisville, Texas).

Animals

All animal work was performed in strict accordance with the Association for Research in Vision and Ophthalmology's statement on the "Use of Animals in Ophthalmic and Vision Research". All protocols were approved by the Institutional Animal Care and Use Committee (IACUC) of the University of Oklahoma Health Sciences Center. Balb/c mice and Sprague-Dawley rats were purchased from Jackson Labs. All animals were maintained in our vivarium on cyclic light (5 lux; 12 h on/12 h off). Experiments were carried out with postnatal day 5 (P5) and 6-week-old male and female mice. We used a minimum of three and maximum of five animals in each experiment.

Plasmids and vectors

We amplified GFP from pcDNA3-GFP-FKHR (Addgene # 9022) using sense (AAGCTT ACC ATG GTG AGC AAG GGC GAG GAG CTG) and antisense (GCGGCCGC GTA GTT GTA CTC CAG CTT GTG CCC CAG) primers and cloned it into pcDNA3 as a Hind III/Not1 fragment. The woodchuck hepatitis virus post-transcriptional regulatory element (WPRE) sequence [8;9] was cloned into pcDNA3 downstream of GFP as a Not1/XhoI fragment. It has previously been shown that the 0.5 kb region immediately 5' of the red pigment gene and the 1.6 kb fragment between 3.0 and 4.5 kb upstream of the red pigment gene are required for cone-specific expression [10]. The human red-cone opsin promoter [10;11] containing the bases spanning -4564 to -3009 and -496 to 0 was amplified by PCR using primers. The -4564 to -3009 fragment was amplified with sense GTC GAC AGG CCT ACA GCA GCC AGG GTG AG and antisense GGATCC AAG AAT GTG AGA CCC AGA AGT GAG CC primers with 5' Stu1 and 3' BamHI sites. The -496 to 0 fragment was amplified with sense GGATCCGAT CCG GTT CCA GGC CTC GGC CCT AAA TAG and antisense GAATTCCATGGCTAT GGA AAG CCC TGT CCC CGC AGG primers with 5' BamHI and 3' EcoRI sites. The two PCR products were cloned into TOPO sequencing vector, and their sequence was verified. The two fragments were excised from the vectors with the respective restriction enzymes, and the two BamHI sites were ligated.

The ligated 2.1 kb fragment was further amplified with sense TCG CGA AGG CCT ACA GCA GCC AGG GTG AG and antisense AGA TCT AAG

CTT CATGGCTAT GGA AAG CCC TGT CCC CGC AGG primers with 5′ Nru1 and 3′ BglII and HindIII restriction sites. After sequence verification, the 2.1 kb red-cone opsin promoter (COP) was excised as Nru1 to BglII, which removes the CMV promoter fragment, and was cloned into pcDNA3 vector. The 225-bp mouse rod opsin (ROP) promoter was provided by Dr. Muayyad Al-Ubaidi, OUHSC. The RPE-specific VMD2 (vitelliform macular dystrophy) promoter construct VMD2-GFP construct was provided by Lea Bennett, OUSHC. The 6.3 kb human red/green opsin promoter construct was provided by Dr. Yun Z. Le, OUHSC. The *Thy-1.2* promoter construct was a gift from Dr. Joshua Sanes (Addgene plasmid # 20736) [12]. The LacZ and TAT-LacZ bacterial expression constructs were kindly provided by Dr. Steven Dowdy, UCSD. The pCAGEN vector (Addgene plasmid # 11160) was a gift from Dr. Connie Cepko [13]. The cDNA encoding NeonGreen [14] (a kind gift from Dr. Martin-Paul Agbaga, OUSHC) was cloned into pCAGEN vector as EcoRI/Not1; this plasmid DNA was called CAG-NeonGreen.

Preparation of liposome protamine/DNA lipoplexes (LPD)

LPD was prepared according to the method reported previously [4], with some modification. First, the liposomes consisting of DOTAP (1, 2-dioleoyl-3-trimethylammonium-propane), DOPE (1, 2-dioleoyl-*sn*-glycero-3-phosphoethanolamine), and cholesterol (1:1:1 molar ratio; Avanti Polar Lipids, Inc., USA) were prepared by thin-film hydration. Second, protamine (1.25 mg/mL; Sigma-Aldrich Co. LLC, USA), peptides (NLS and TAT; 0.5 mg/mL), and the plasmid DNA (pDNA) were mixed at various weight ratios (Table 1). Using a 1:20 DNA to liposome ratio resulted in the best gene expression among all DNA to liposome ratios tested. The resultant protamine/pDNA complex was allowed to stand at room temperature for 20 min. The above liposome was then added into the protamine/pDNA complex, followed by vortexing. The resultant mixture was kept at room temperature for another 20 min to form liposome/ protamine/ DNA lipoplexes.

Intravitreal injection

For intravitreal injections, the animals were anesthetized with an intraperitoneal injection of ketamine (80-100 mg/kg) and xylazine (5 mg/kg). The eyes were injected with 1 µl (~ 85 ng of DNA) of LPD nanoparticles using a 33-gauge needle. Animals were monitored daily for signs of infection or cataracts, and were euthanized if either occurred. At the end of the experiment, the mice were killed and the eyes were processed for microscopic analysis.

Table 1: Formulation of lipid-based nanoparticles (LPD) for *in vivo* application.

Weight/Volume DNA: Liposome Ratio	DNA	Protamine	NLS	Liposome (1M)
1:05	8 µg	8 µg	24 µg	8 µl
1:07	8 µg	8 µg	24 µg	11.2 µl
1:09	8 µg	8 µg	24 µg	14.4 µl
1:12	8 µg	8 µg	24 µg	19.2 µl
1:15	8 µg	8 µg	24 µg	24 µl
1:20	8 µg	8 µg	24 µg	32 µl
DNA: Protamine Ratio 1:1				
DNA: NLS Ratio 1:3				

LPD was prepared according to the method reported previously [6]. DOTAP, DOPE, and cholesterol (1:1:1 molar ratio) were prepared by thin-film hydration. Protamine (1.25 mg/m), peptides (NLS and TAT; 0.5 mg/mL) and the plasmid DNA (pDNA) were mixed at various weight ratios. Using a 1:20 DNA to liposome ratio resulted in the best gene expression among all DNA to liposome ratios tested.

Subretinal injection

Intravitreal injection is ideal to target ganglion cells, but is not ideal to transduce genes to photoreceptor cells and retinal pigment epithelium. The subretinal injections were performed *via* the transscleral route. Mice were anesthetized by intramuscular injection of a ketamine (80-100 mg/kg) and xylazine (5 mg/kg) mixture of approximately 0.1 ml, until mice did not display a blink reflex to a touch on the corneal surface. Eyes were dilated with 1% cyclopentolate hydrochloride ophthalmic solution applied to the cornea (Akron, Lake Forest, IL). The mice were kept on a 37°C regulated heating pad under a surgical microscope (Carl Zeiss Surgical, NY). An insulin syringe with a beveled 30-gauge needle was used to puncture a hole in the cornea. Next, a 33-gauge blunt-end needle attached to a 10-µl Nanofil® syringe controlled by a UMP3 pump controller (World Precision Instruments, Sarasota, FL) was positioned toward the superior nasal portion of the retina. Then, 1 µl of LPD nanoparticles (~85 ng of DNA) were injected into the subretinal space. The needle was retracted 10–15 s after injection, when a bleb of retinal detachment was visible. Following complete removal of the injection needle, the eye was carefully observed for any indication of post-surgical complications, such as iris and sub-retinal bleeding, pronounced retinal detachment or damage, or excessive vitreous loss. After injection, saline and GelTeal lubricant eye gel (Alcon, Fort Worth, TX) were applied topically to the eye 3-4 times daily for 3-4 days after injection, to keep the eye continually moist. The severity of acute post-surgical complications and subsequent long-term complications, including eye infection, loss of visual function, and atrophy, were carefully evaluated to determine whether the animal would be excluded from the study. In the absence of any severe complications, the procedure was deemed successful and the animal remained in the study.

Purification of TAT- fusion proteins

E.coli BL21 (DE3) with the recombinant plasmid was grown to a stationary phase at 37°C in LB medium containing ampicillin (100 µg/ml) and a final concentration of 1 mM isopropyl β-D-galacto-pyranoside (IPTG). The bacteria were harvested by centrifugation at 10,000 x g for 10 min. The bacteria were suspended in buffer A (50 mM Tris-HCl, pH 8.0 containing 100 µg/ml lysozyme, 2 mM EDTA, 1 mM phenylmethylsufonyl fluoride, 0.5 µg/ml leupeptin, 0.1% Triton X-100, 10 mM $MgCl_2$, and 10 µg/ml DNase). The bacterial suspension was incubated for 30 min on ice. The lysate was cleared by centrifugation at 15,000 x g for 20 min. The pellet was discarded. The supernatant was loaded onto a Ni^{2+}-NTA agarose (super flow) affinity column equilibrated with 10 mM imidazole. This was followed by elution with 500 mM imidazole.

Transmission electron microscopy (TEM)

The morphology of LPD was observed using TEM (Carl Zeiss, Germany). One drop of LPD or LPD complexed with TAT peptide was placed on a copper grid. The samples were negatively stained with 1% uranyl acetate. The grid was allowed to dry further for 20 min and was then examined with the electron microscope, as we described previously [15].

Fundus imaging

Mice were anesthetized with an intraperitoneal injection of ketamine (80-100 mg/kg) and xylazine (5 mg/kg) to prevent large movements during the fundoscopy (Micron III fundoscope). Both pupils were dilated using a topically applied drop of tropicamide (1%) to neutralize corneal optical power and focus the fundoscope onto the retina. Hydroxymethylcellulose ophthalmic demulcent solution (Goniosol 2.5%) was placed on the cornea to preserve corneal hydration and to couple the objective to the cornea. Mice were secured on a custom stage that allowed for free rotation, in order to align the eye for imaging of the optic nerve head. Images were taken using Bright field or GFP filters. Images were further processed in Adobe Photoshop CS5.

Immunostaining of RPE and retinal whole-mounts

Eyes were enucleated and placed in cold Hanks' Balanced Salt Solution buffered with 25 mM HEPES (pH 7.2), after which the cornea and lens were removed and the retina and RPE were carefully isolated. Relaxing cuts were made in the retinal margins. The whole retinas or RPE were flattened onto a black filter membrane. Whole-mounted retinas were fixed in 4% paraformaldehyde in PBS at 4°C for 2 h, and were rinsed in PBS. Intrinsic fluorescence or labeling in retinal and RPE whole-mounts was imaged using either a Nikon Eclipse E800 (Tokyo, Japan), an Olympus IX70, or an Olympus MVX10 (Olympus USA, Center Valley, Pennsylvania) microscope.

Primary culture of retinal neurons

Timed pregnant Sprague-Dawley® rats were ordered each week. The retinas of 10-15 0-to-2-day-old pups were removed with a dissecting microscope under sterile conditions in a tissue culture hood. The retinas were suspended in 25 ml of Dulbecco's Modified Eagle's Medium (DMEM) with F-12 medium plus 10% fetal calf serum in a plastic bag, and were mechanically dissociated for 2 min using a Stomacher set on low power. The suspension was first filtered through a 230-µm sieve, which was then rinsed once with medium. The combined filtrates were passed through a 140-µm sieve, followed by a rinse with undiluted fetal calf serum. The filtered suspension was centrifuged at 800 rpm for 5 min in a clinical centrifuge. The supernatant was decanted, and the cell pellets were resuspended in 25 ml of media using a sterile 5-ml pipette. Cell concentration was determined with a cell counter or hemocytometer. The suspension was diluted with medium to 1×10^5 cells/ml. The cells (1 ml) were plated in 24-well tissue culture plates on 12-mm coverslips that had been pretreated overnight with 10 µg/ml poly-D-lysine. The cells were maintained in DMEM with F-12 medium and 2% fetal calf serum, or in synthetic serum-free media. The cultures were used in experiments 7-10 days after plating.

Results

Protein transduction domains (PTD) enhanced transduction potential *in vitro*

The cDNA open reading frame of LacZ (β-galactosidase) was cloned in-frame downstream of an N-terminal leader composed of a six-histidine-residue purification tag, followed by the presence or absence of TAT-PTD sequence (YGRKKRRQRRR; Fig. 2A). The recombinant proteins were expressed in bacteria and purified to apparent homogeneity on a Ni^{2+}-NTA chromatography column (Fig. 2B). To determine the transduction efficiency of TAT-PTD, we prepared primary retinal neurons from rat retinas, and incubated these with purified TAT-LacZ or LacZ proteins for 30 min. The cells were then washed with PBS. LacZ enzyme activity was assessed by X-Gal staining [16]. The neurons treated with TAT-LacZ showed strong LacZ activity, while neurons treated with LacZ lacking TAT-PTD did not

(Fig. 2C,D). This finding suggests that the TAT-PTD sequence efficiently transduced the proteins *in vitro*. The absence of LacZ activity in LacZ-treated neurons was not due to enzyme inactivation, but was caused by lack of internalization, as both purified LacZ and TAT-LacZ had similar enzyme activity *in vitro* (Fig. 2E).

## Morphological characteristics of LPD nanoparticles complexed with TAT peptide

The morphology of LPD and LPD complexed with TAT peptide was observed using TEM. The sizes of the LPD and LPD complexed with TAT peptide ranged from 80-120 nm (Fig. 3). The results show that addition of TAT peptide did not change the size or morphology of LPD.

Protein transduction domains enhanced transduction potential *in vivo*

We examined the efficacy of lipid nanoparticles in the delivery of GFP plasmid DNA to the retina. We complexed LPD, with or without TAT or NLS peptides (Fig. 4). Control experiments were done with liposome and protamine without plasmid DNA. Four-week-old Balb/c mice were subretinally injected with LPD nanoparticles with the above combinations. GFP fluorescence was examined two and seven weeks later using fundoscopy to visualize the interior surface of the eye. Our results clearly suggest that LPD combined with NLS enhances the expression of GFP; in combination with TAT, the expression is even stronger (Fig. 4). Interestingly, at seven weeks after injection, the GFP expression was much stronger than it was at two weeks after injection, suggesting that LPD facilitates longer sustainability of gene expression.
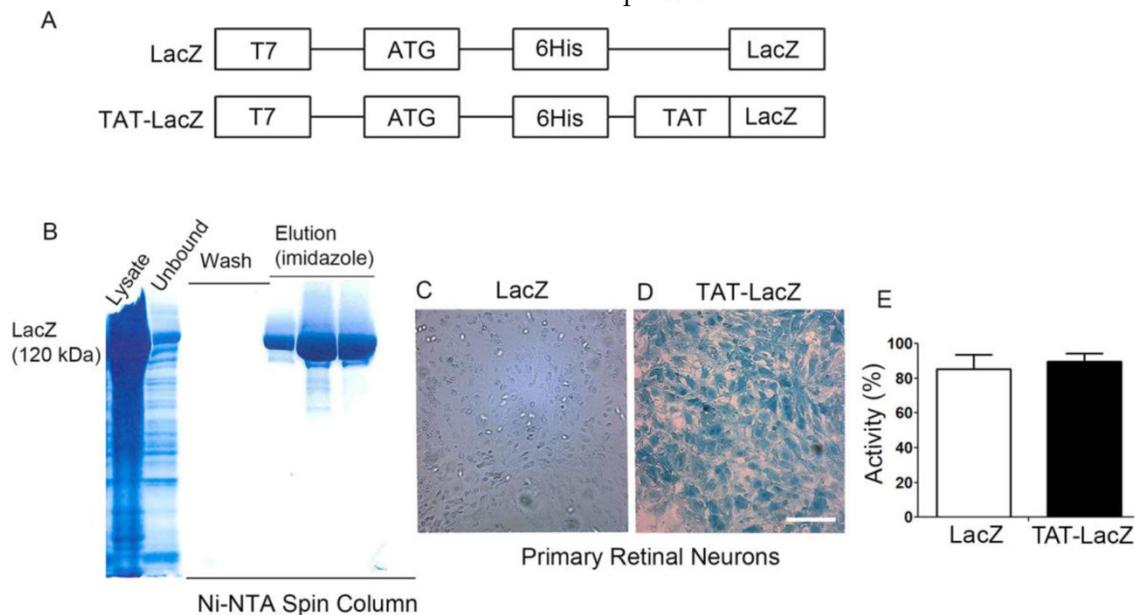
Figure 2. Effect of TAT-epitope on the internalization of proteins. Schematic illustration of LacZ and TAT-LacZ plasmid DNAs used in this study (**A**). Proteins were expressed in the bacteria, and affinity purified on a Ni^{2+}-NTA super flow affinity column chromatograph. Various fractions of the column (lysate, unbound, wash, and eluted fractions) were subjected to SDS-PAGE, followed by Coomassie blue staining to visualize the proteins (**B**). Transduction of LacZ and TAT-LacZ proteins into the retinal primary neurons in culture. Analysis of LacZ enzyme activity assays by X-Gal staining after 30 min of incubation (**C,D**). Scale bar: 200 µm. To determine the effect of TAT on LacZ activity, equal amounts of (63 ng) TAT-LacZ and LacZ proteins were used to measure LacZ activity (**E**).
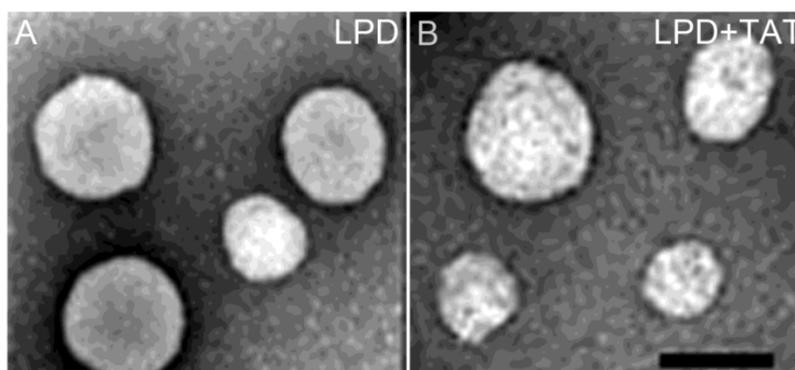
Figure 3. Morphology of LPD observed with transmission electron microscopy (TEM). The LPD (**A**) and LPD complexed with TAT peptide (**B**) were negatively stained with 1% uranyl acetate and visualized under TEM. Scale Bar: 100 nm.
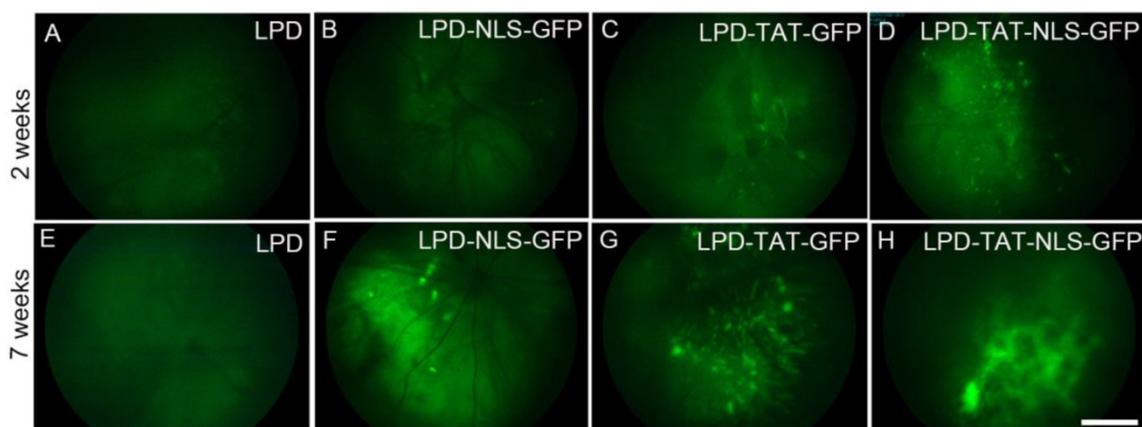
Figure 4. Effect of TAT on the *in vivo* transfection by LPD. Plasmid DNAs of either control plasmid (LPD with pcDNA3 vector) or GFP were complexed with LPD in the presence or absence of TAT or NLS, or a combination of TAT and NLS, and injected subretinally into Balb/c mice. Fluorescent fundoscopy images of the eye were taken two and seven weeks after injection. Scale bar: 100 µm.

LPD-mediated RPE cell–specific expression

To determine the RPE cell-specific expression of LPD *in vivo*, we used RPE (Vitelliform macular dystrophy, VMD2) cell-specific promoter. Plasmid DNAs of pcDNA3 (control) or VMD2-GFP were individually complexed with LPD and subretinally injected into Balb/c mice. One week later, fundoscopy was performed on the mice. Mouse eyes were harvested and subjected to RPE and retinal flat mount preparation. RPE and retinal flat mounts were then examined for GFP expression. GFP expression was observed in RPE, but was barely detectable in the retina (Fig. 5A and B).

Retinal pigment epithelium protein 65 (Rpe65) is an RPE-specific protein [17]. We stained both RPE and retinal flat mounts with Rpe65 antibody. We observed Rpe65 expression in RPE, while Rpe65 was barely detectable in the retina (Fig. 5D and E). To examine the specificity of Rpe65 antibody towards Rpe65 protein, we stained RPE flat mounts prepared from Rpe65$^{-/-}$ mice. The results showed a complete absence of Rpe65 expression in RPE from Rpe65$^{-/-}$ mice (Fig. 5F). When we merged the images of GFP and Rpe65, the merged images indicate a co-localization of VMD2-GFP with Rpe65 protein in the RPE (Fig. 5G) and the absence of GFP and Rpe65 expression in the retina (Fig. 5H). These findings suggest an LPD-mediated RPE cell–specific expression of GFP under the control of RPE cell-specific promoter.

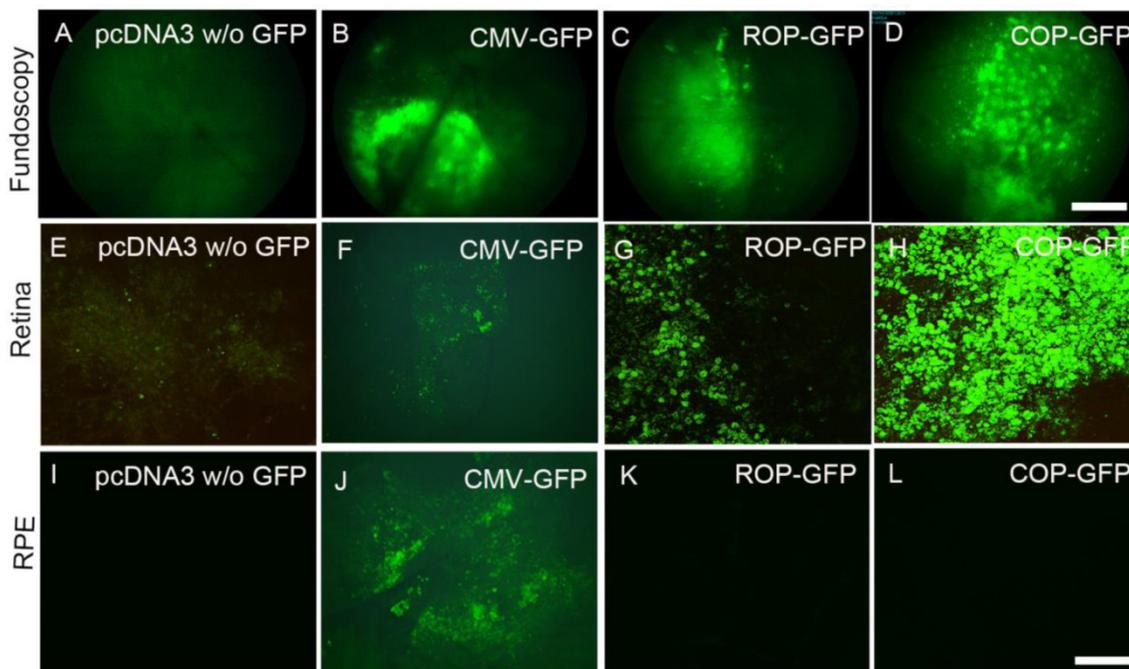## LPD-mediated rod- and cone-cell–specific expression

To achieve rod and cone cell-specific expression, we cloned GFP under the control of mouse rod opsin promoter (ROP). To achieve cone cell-specific expression, we cloned GFP under the control of human red/green cone opsin promoter (COP). Plasmid DNAs of pcDNA3 (control), ROP-GFP, and COP-GFP were individually complexed with LPD and subretinally injected into Balb/c mice. We previously reported that CMV-promoter drives reporter gene expression in the RPE, and we used this construct as a positive control [6]. One week later, fundoscopy was performed on the mice. The results revealed the expression of GFP in CMV-GFP-, ROP-GFP-, and COP-GFP-injected mice, but no GFP expression in pcDNA3 control mice (Fig. 6A-D). Analysis of GFP expression on retinal and RPE flat mounts indicated that ROP and COP drive the expression of GFP in the retina (Fig. 6 G, H), but not in the RPE (Fig. 6 K, L). However, the CMV-promoter drives increased expression of GFP in the RPE (Fig. 6J) compared with the retina (Fig. 6F). These experiments suggest an LPD-mediated rod and cone cell–specific expression of GFP under the control of rod and cone cell-specific promoters.

To determine the cell-specific expression of GFP in rod and cone cells, we labeled prefer-fixed retinal sections of pcDNA3, ROP-GFP, and COP-GFP with cone-specific marker peanut agglutinin (PNA), which labels cone outer segments, and examined the sections for fluorescence. We observed no GFP fluorescence in pcDNA3-injected mouse retinas, but observed PNA staining in the cones (Fig.7A,D). Both ROP-GFP- and COP-GFP-injected mouse retinal sections expressed GFP fluorescence (Fig. 7B,C). However, PNA co-labeled with GFP in cones (Fig. 7I), but not in rods (Fig. 7H). Collectively, these data show that LPD efficiently delivers genes in a cell-specific manner under the control of cell-specific promoters.
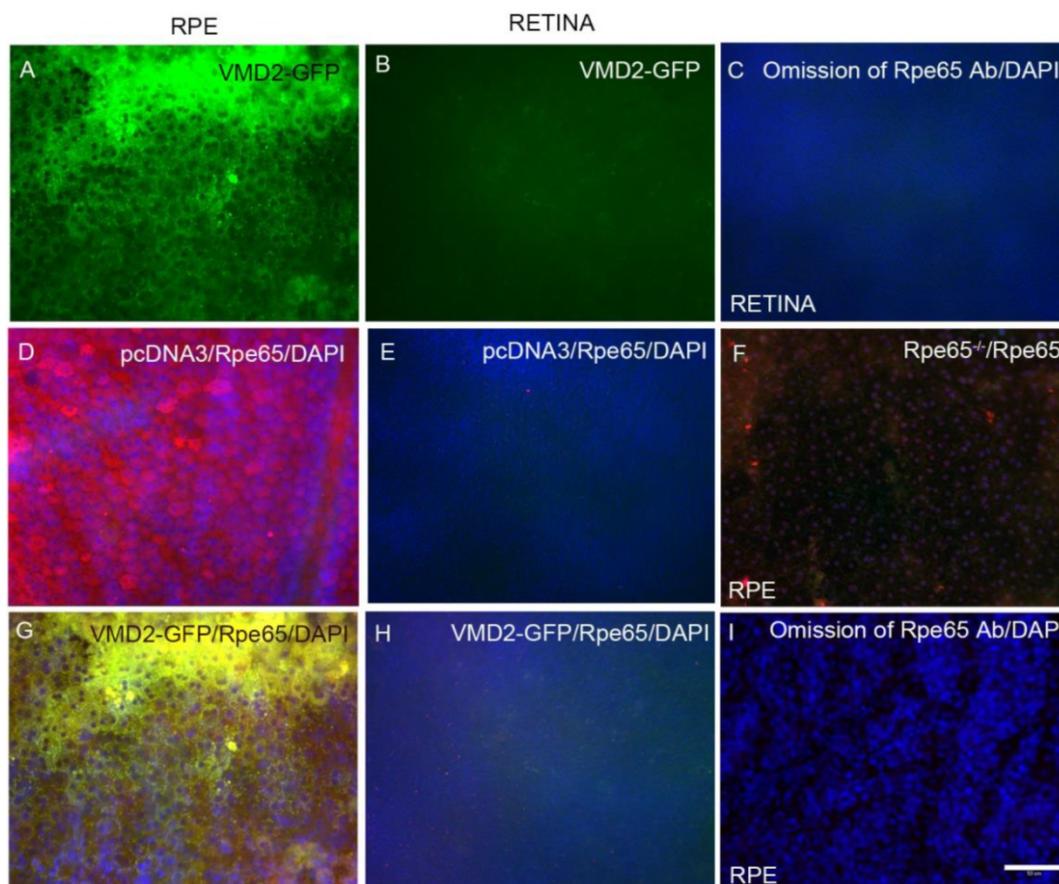
Figure 5. LPD-mediated retinal cell-specific expression by Rpe-specific VMD2 promoter. Plasmid DNAs of either control (pcDNA3 vector) or vector carrying GFP under the control of VMD2 were complexed with LPD and subretinally injected into Balb/c mice. One week later, RPE (**A, D, G, F, I**) or retinal (**B, C, E, H)** flat mounts were prepared and examined under microscopy for fluorescence or stained with Rpe65 antibody (**D, E, F, G**). Scale bar: 50 μm. Panel **F** represents the RPE flat mount from Rpe65^{-/-} mice stained with Rpe65 antibody (control for Rpe65 expression).

Figure 6. LPD-mediated retinal cell-specific expression by rod cell-specific mouse rhodopsin promoter (ROP) and cone cell-specific cone-opsin promoter (COP). Plasmid DNAs of either control (pcDNA3 vector) or vector carrying GFP under the control of CMV, ROP, or COP were individually complexed with LPD and subretinally injected into Balb/c mice. One week later, fluorescent fundoscopy images of the eye were taken (A-D), followed by retinal (E-H) or RPE flat mounts (I-L) that were prepared and examined under microscopy for fluorescence. We included CMV-GFP (B, F, J) as a positive control, since CMV-promoter drives the expression in RPE (J) compared with the retina (F). Panels A, E, I represent the LPD-mediated transfection of pcDNA vector without (w/o) carrying GFP. Scale bar: A-D, 100 μm; E-L, 50 μm.
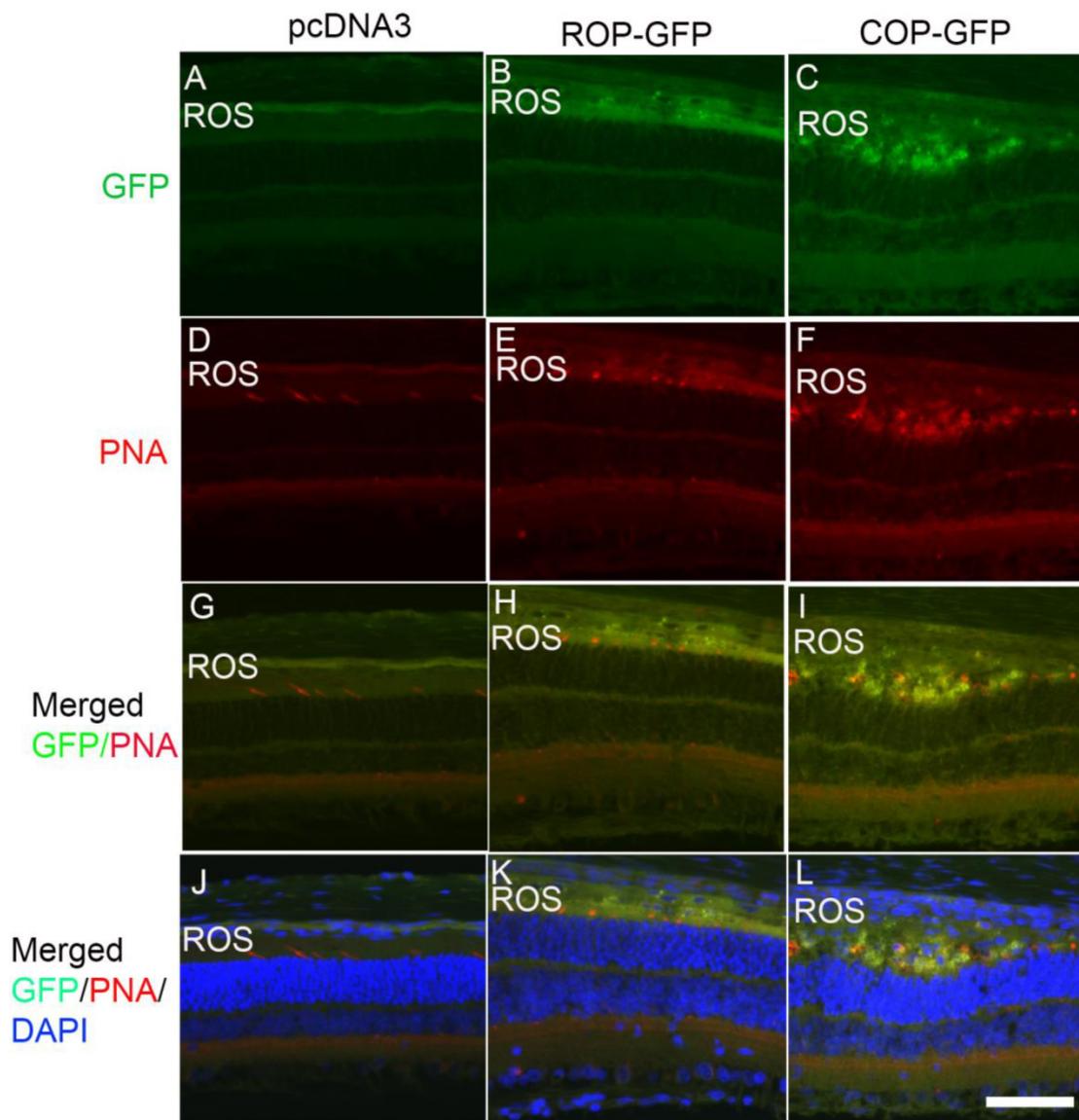
Figure 7. Analysis of LPD-mediated photoreceptor cell-specific gene expression. We incubated prefer-fixed sections of LPD-pcDNA3- (**A, D, G, J**), LPD-pcDNA3-ROP-GFP- (**B, E, H, K**), and LPD-pcDNA3-COP-GFP- (**C, F, I, L**) injected eyes from Balb/c mice with peanut-agglutinin (PNA), which labels the cone outer segments, and examined the GFP fluorescence under fluorescence microscopy. Panels **A-C** represent GFP fluorescence; panels **D-F** represent PNA labeling of cones; panels **G-I** represent co-labeling of GFP/PNA, and panels **J-L** represent co-labeling of GFP/PNA and DAPI to visualize nuclei. ROS, rod outer segments. Scale bar: 50 µm.

Efficient LPD-mediated delivery of plasmid DNAs into retinal ganglion cells

We constructed a gene delivery vector specifically targeting retinal ganglion cells (RGCs). The promoter contains 6.5 kb of the murine *Thy-1.2* gene, extending from the promoter to the intron following exon 4, but lacking exon 3 and its flanking introns. The deleted sequences are required for expression in non-neural cells, but not in neurons, whereas sequences in upstream introns are required for expression in neurons (Fig. 8A). We cloned the GFP sequence into an *Xho1* site, replacing the deleted sequences. We transfected the *Thy1.2*-GFP construct into HEK-293T cells, and intravitreously injected the construct complexed with LPD into Balb/c mice.

Seventy-two hours later, GFP fluorescence was examined in HEK-293T cells and retinal flat mounts. We co-labelled RGCs with Brn-3a, a ganglion cell marker. We observed no expression of GFP driven by *Thy-1.2* promoter in HEK-293T cells (Fig. 8 B-D). However, GFP driven by *Thy-1.2* promoter was expressed in RGCs and was co-localized with Brn-3a on retinal flat mounts (Fig. 8. H-K).

To specifically determine the ganglion cell-specific expression of GFP, we labeled cryosections of pcDNA3 and *Thy1.2*-GFP sections with Brn-3a (Fig. 9B and F), and examined the sections for fluorescence (Fig. 9A and E). We observed no GFP fluorescence in pcDNA3-injected mouse retinas (Fig. 9A), but observed fluorescence in the ganglion cell

layer (Fig. 9E). The Brn-3a expression co-localizes with GFP in the ganglion cell layer (Fig. 9G). Collectively, these data show that LPD under the control of a ganglion cell-specific promoter efficiently delivers genes to ganglion cells.

Efficient LPD-mediated delivery of plasmid DNAs under the control of CAG promoter

We cloned a cDNA encoding NeonGreen fluorescent protein under the control of a CAG promoter. CAG promoter contains a cytomegalovirus (CMV) early enhancer element, the promoter, the first exon and the first intron of chicken beta-actin gene, and the splice acceptor of the rabbit beta-globin gene [18;19]. The NeonGreen plasmid DNA was complexed with LPD and injected subretinally into mice. One week later, retina and RPE flat mounts were prepared and NeonGreen fluorescence was examined. The results indicate a high level of expression of NeonGreen in the retina, but not in the RPE (Fig. 10G-I).
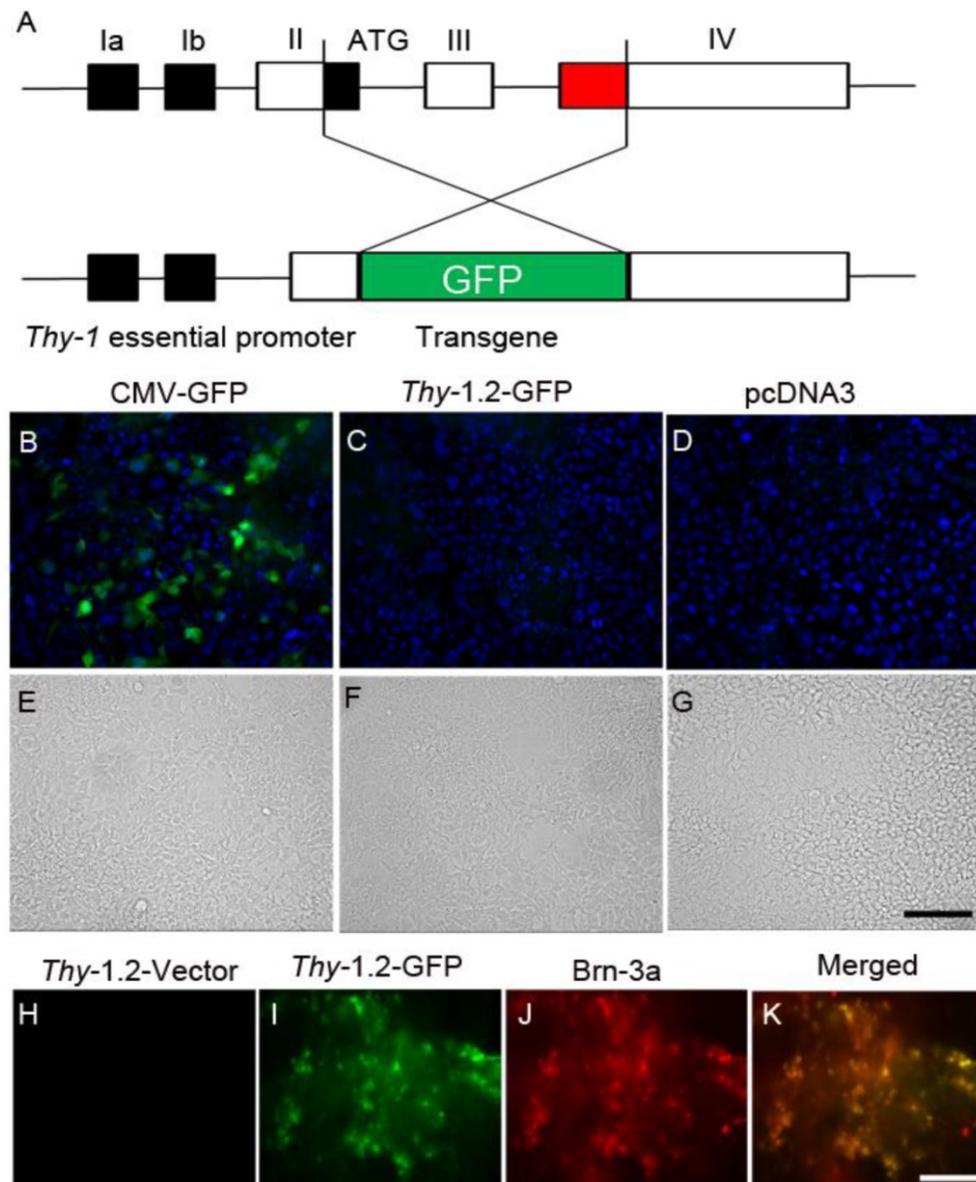

Figure 8. LPD-mediated gene delivery to retinal ganglion cells. Schematic representation of the *Thy-1.2*-driven GFP expression cassette. The promoter contains 6.5 kb of the murine *Thy1.2* gene. Exon 3 is required for expression in non-neural cells, but not in neurons. We cloned the GFP sequence into an *XhoI* site, replacing exon 3. Exons 1 through 4 are shown in the diagram (**A**). Expression of GFP driven by CMV and *Thy-1.2* promoters in HEK-293T cells. Expression constructs of GFP driven by CMV (**B**) and *Thy-1.2* (**C**) promoters were transfected into HEK-293T mammalian cells. CMV-pcDNA3 plasmid (**D**) was used as a negative control. Cells were examined for fluorescence 72 h after transfection. DAPI was added to cells to visualize nuclei (blue). Panel **E-G** represents bright-field light images of **B-D**. Plasmid DNAs of either *Thy-1.2* vector or *Thy-1.2*-GFP were complexed with LPD and injected intravitreously into Balb/c mice. One week later, retinal flat mounts were prepared and examined for GFP expression (**H, I**), or co-labelled with a ganglion cell maker, Brn-3a (**J**). Panel **K** represents a merged image of GFP and Brn-3A. Scale bar: 50 μm.
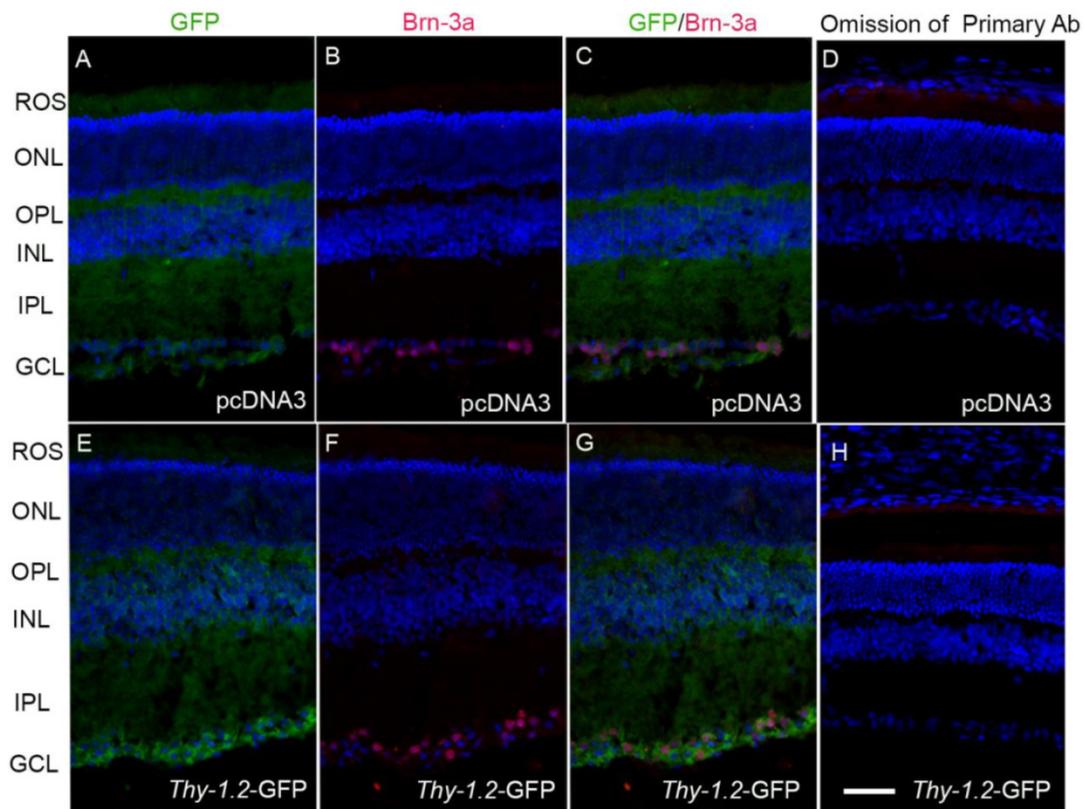
Figure 9. Analysis of LPD-mediated ganglion cell-specific gene expression. We incubated prefer-fixed sections of LPD-pcDNA3- (**A-D**) or LPD-Thy*1.2*-GFP- (**E-H**) injected eyes from Balb/c mice and stained the sections with Brn-3a and GFP antibodies. Panels **A** and **E** represent GFP fluorescence; panels **B** and **F** represent Brn-3a labeling of ganglion cells; panels **C** and **G** represent merge images of GFP and Brn-3a; panels **D** and **H** represent the omission of primary antibodies. Nuclei were stained with DAPI. Scale bar: 50 µm. ROS, rod outer segments; ONL, outer nuclear layer; OPL, outer plexiform layer; INL, inner nuclear layer; IPL, inner plexiform layer; GCL, ganglion cell layer.
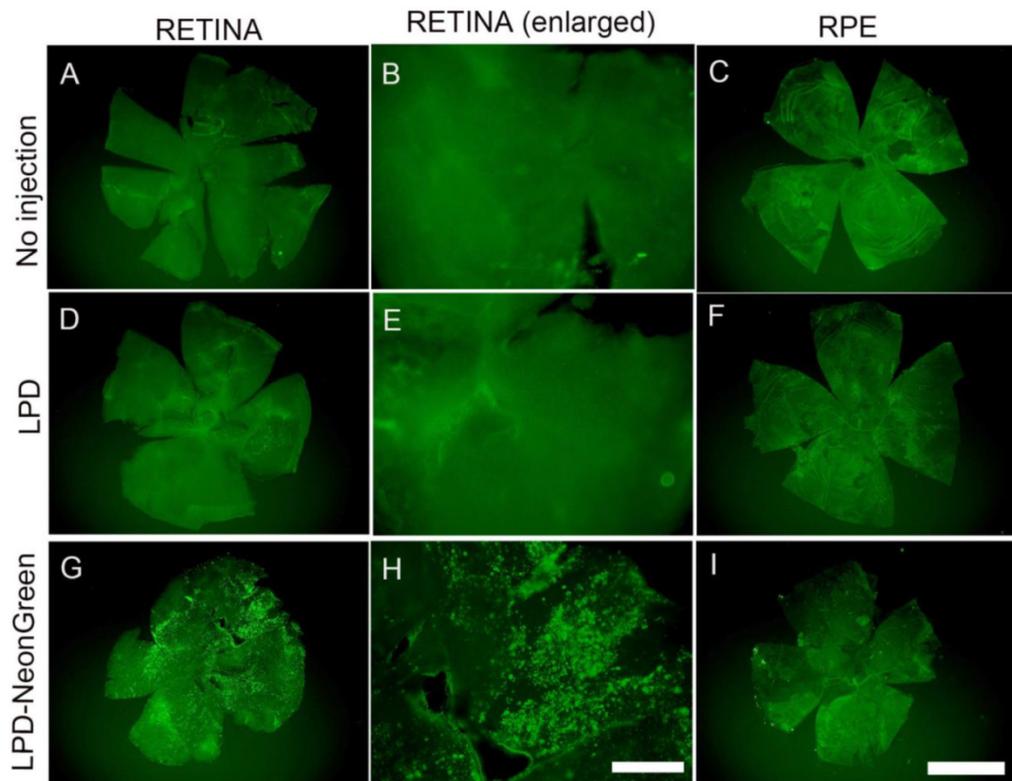
Figure 10. LPD-mediated gene delivery under the control of CAG promoter. NeonGreen plasmid under the control of CAG promoter was complexed with LPD and injected subretinally into Balb/c mice. Controls include no injection and LPD without NeonGreen. One week later, retinal (**A, D, G**) and RPE (**C, F, I**) flat mounts were prepared. We examined fluorescence as a function of NeonGreen expression. A region of the retinal flat mount was enlarged (**B, E, H**). Scale bar: **A, C, D, F, G, I:** 1 mm; **B, E, H:** 200 µm.
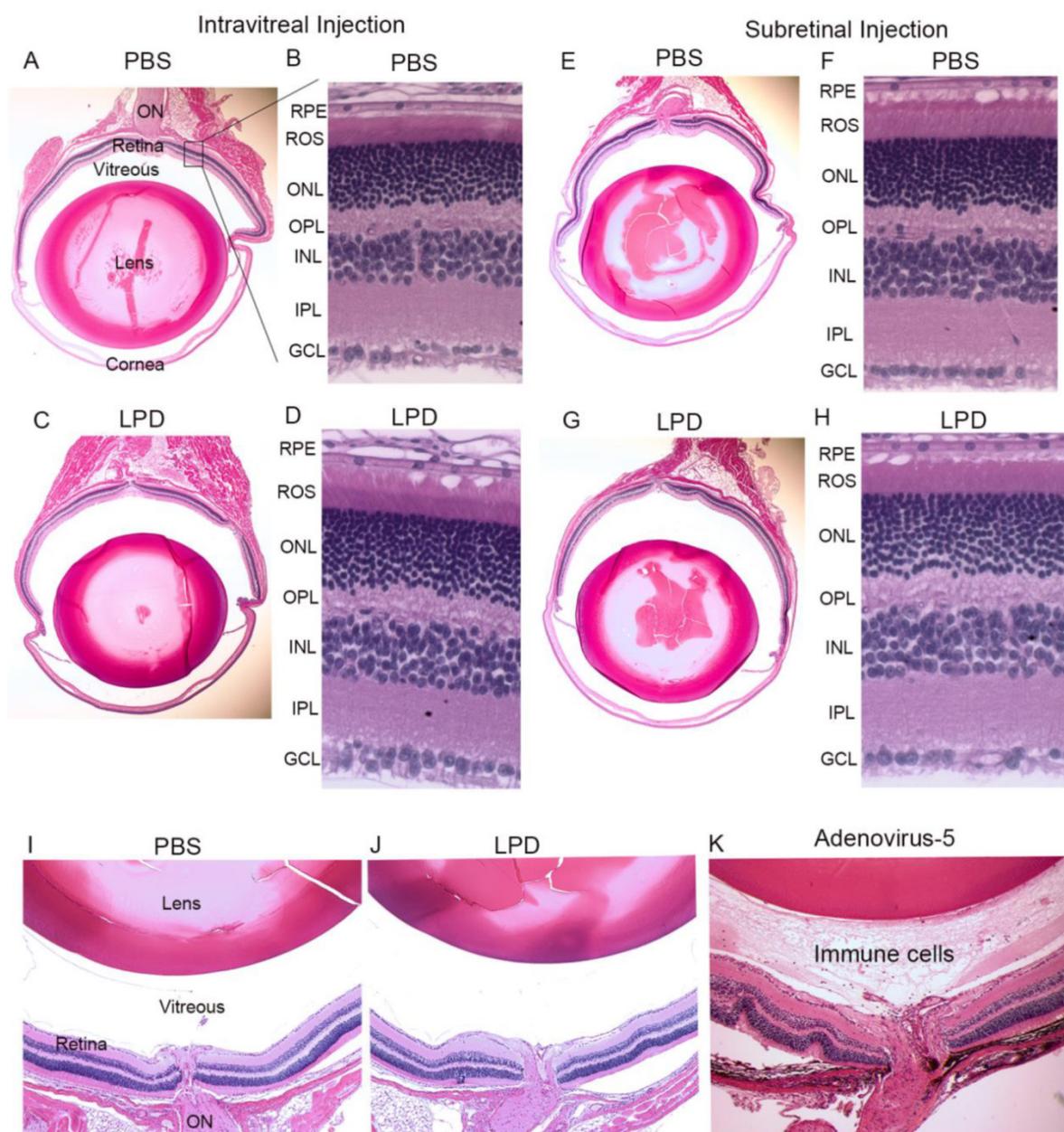
Figure 11. Effect of LPD on retinal structure. To examine whether LPD has a deleterious effect on retina structure, PBS or LPD was injected into Balb/c mice intravitreally (**A, B, C, D**) or subretinally (**E, F, G, H**). Five-micrometer-thick sections of retinas were cut along the vertical meridian and stained with hematoxylin and eosin (**A, C, E, G**). A region of the retina near the optic nerve head was enlarged for fine details (**B, D, F, H**). A region around the optic nerve head was imaged to examine for any immune cells. Panel **I** represents the intravitreally PBS-injected eye, and panel **J** represents the intravitreally LPD-injected eye. Mouse eyes injected with Adenovirus 5 (Ad5) were used as a positive control for inflammation. Immune cells were observed in the vitreous of the Ad5-injected eye (**K**). RPE, retinal pigment epithelium; ROS, rod outer segments; ONL, outer nuclear layer; OPL, outer plexiform layer; INL, inner nuclear layer; IPL, inner plexiform layer; GCL, ganglion cell layer.

Effect of LPD on retina structure

To examine whether LPD has a deleterious effect on retinal structure, PBS or LPD was subretinally or intravitreally injected into Balb/c mice. One week after injection, mice underwent electroretinography (ERG). After ERG, mice were killed with an overdose of carbon dioxide. Five-micrometer-thick sections of retinas were cut along the vertical meridian and stained with hematoxylin and eosin to permit examination of the retina (Fig. 11). A region of the retina near the optic nerve head was enlarged for fine details (Fig. 11A). The results showed that there was no difference in the morphology of the retina after PBS and LPD injection, and no difference after either subretinal or intravitreal injection (Fig. 11B,D,F,H). The results also suggested that there was no inflammation in the vitreous cavity in either PBS- or LPD-injected eyes (Fig. 11 A, E, C, G). For positive control of inflammation, we intravitreally injected adenovirus 5, and we found the presence of immune cells in the vitreous cavity (Fig. 11K).

Discussion

Our current work represents the promising application of biocompatible lipid-based non-viral nanoparticles to achieve eye cell type-specific gene transfer to develop gene therapy strategies for treating blinding eye diseases. As a proof of principle, the LPD complexed with genes under the control of retinal cell-specific promoters produced cell-specific expression of the reporter gene. The formulated lipid nanoparticles may be appropriate for use with other tissues, for the purposes of gene delivery with tissue-specific promoters.

In the present study, we did not compare our approach with surface-engineered viral vectors [20]. However, our previous publications reported that Rpe65 gene delivery to Rpe65 knockout mice is comparable to AAV [21] and lentiviral [22] gene transfer of Rpe65 to *Rpe65* knockout mice. Despite the promise associated with the use of viral vectors in gene therapy, there are also significant risks. These risks include the possibility that a virus may recover its ability to cause disease once inside the body and the possibility of immune and inflammatory responses whenever any foreign particle, such as a virus, is introduced into the body. We have not observed any inflammatory response in response to LPD administration to the eye. We found that LPD has no effect on the retinal structure (Fig. 11) or visual function (data not shown), consistent with our earlier findings that subretinal injection of LPD nanoparticles with target genes significantly rescued the visual function in blind mice [6]. The advantages are that LPD nanoparticles are biocompatible and the particles are stable, as demonstrated indirectly by gene expression, in addition to long-term expression of the gene by a single administration. LPD demonstrates much lower gene expression than does viral-mediated gene delivery. This may be a limitation. However, this lower level of expression did not affect the rescue of retinal function in Rpe65 gene delivery [6]. We generally administer 1-1.5 µl of LPD nanoparticles, which contains ~85 ng of DNA, per eye. Further studies should aim to increase the amount of DNA to boost gene expression. However, overexpression of genes to photoreceptors may cause retinal degeneration [23].

In the current study, we showed RPE and retinal cell expression by a ubiquitous CMV promoter. Surprisingly, the same promoter in the CAG vector [13], drives the expression of the reporter gene only in the retina but not in the RPE (Fig. 10). This deviation from its ubiquitous nature could be attributable by the presence of a human beta-globin intron in the CAG vector (Fig. 10) and is absent from the CMV-GFP vector (Fig. 6). In a recent study, CMV vector carrying the human beta-globin intron was used to target anti-oxidant genes to photoreceptor cells [24]. Intravitreal injection is ideal to target ganglion cells, but transfection of different retinal cells has been achieved after both types of administrations, subretinal and intravitreal. Generally, intravitreal administration of genes driven by a ubiquitous promoter should be able to diffuse to the retina. Therefore, the intravitreal administration could be an advantage over subretinal injection [20]. Since the efficiency of LPD is lower than the viral mediated approach, subretinal injection would be an ideal route for LPD-mediated RPE and photoreceptor cell expression. In the present study, we also cloned the woodchuck hepatitis virus post-transcriptional regulatory element (WPRE) sequence [8;9] downstream of GFP, which is known to increase the gene expression.

Cell-targeting and cell-internalization peptides have been extensively used for efficient drug delivery and for image analysis [4;5]. A peptide derived from TAT-protein from human immunodeficiency virus (HIV)-1, has been utilized to deliver exogenous proteins that translocate through the cell membranes and accumulate in the nucleus [25]. These protein transduction domains have been extensively used for the delivery of biologically active proteins *in vivo* [26-28] , and protein therapy has been used as a treatment for various diseases [29-31]. In the present study, we found that TAT peptide enhanced LPD-mediated gene delivery *in vivo*.

The current study has significantly contributed to findings regarding the therapeutic potential of this approach for treating a variety of retinal degenerative diseases. Among these, age-related macular degeneration (AMD) is an eye disease primarily affecting the central vision in people ages 60 and older [32;33]. In AMD, light-sensing rod and cone photoreceptor cells do not function over time [32;33]. Age and disease-related structural changes in the RPE have been reported in AMD [34;35]. Retinitis pigmentosa (RP) is the most common inherited cause of blindness in people between the ages of 20 and 60 worldwide [36]. In RP, rods are affected, followed by cone photoreceptors [37]. Diabetic retinopathy (DR) is the most common disorder affecting cones [38;39]. Retinal ganglion cell (RGC) survival is critical for vision, and injury to RGC axons in the optic nerve may lead to rapid RGC death [40;41]. Progressive RGC cell death is known to occur in optic neuropathy, optic neuritis, and glaucoma [40;41]. In the present study, we tested the LPD-mediated delivery of genes to RPE cells, rod cells, cone cells, and ganglion cells. This work will help in targeting therapeutic genes in the retinal diseases described above.

Conclusions

Our studies clearly show that LPD could be used to deliver a functional gene to the retina. To demonstrate cell specificity to circumvent off-target effects in the future, we achieved retinal pigment epithelium, rod, cone, and ganglion cell-specific expression with retinal cell-specific promoters. This work will inspire investigators in the field of lipid nanotechnology to couple cell-specific promoters to drive expression in a cell- and tissue-specific manner. Our study demonstrated for the first time that cell-specific promoters could enable lipid-based nanoparticles to deliver genes to specific cells of the retina *in vivo*.

Abbreviations

LPD, lipid nanoparticles; CMV, cytomegalovirus; RP, retinitis pigmentosa; RPE, retinal pigment epithelium.

Acknowledgements

Competing Interests

The authors claim no competing financial interests.

References

1. Mashaghi S, Jadidi T, Koenderink G, Mashaghi A. Lipid nanotechnology. International Journal of Molecular Sciences. 2013; 14: 4242-4282.
2. Li S, Rizzo MA, Bhattacharya S, Huang L. Characterization of cationic lipid-protamine-DNA (LPD) complexes for intravenous gene delivery. Gene Therapy. 1998; 5: 930-937.
3. Li S, Huang L. In vivo gene transfer via intravenous administration of cationic lipid-protamine-DNA (LPD) complexes. Gene Therapy. 1997; 4: 891-900.
4. Ma K, Wang DD, Lin Y, Wang J, Petrenko V, Mao C. Synergetic Targeted Delivery of Sleeping-Beauty Transposon System to Mesenchymal Stem Cells Using LPD Nanoparticles Modified with a Phage-Displayed Targeting Peptide. Advanced. Functional Materials. 2013; 23: 1172-1181.
5. Abbineni G, Modali S, Safiejko-Mroczka B, Petrenko VA, Mao C. Evolutionary selection of new breast cancer cell-targeting peptides and phages with the cell-targeting peptides fully displayed on the major coat and their effects on actin dynamics during cell internalization. Molecular Pharmaceutics. 2010; 7: 1629-1642.
6. Rajala A, Wang Y, Zhu Y, Ranjo-Bishop M, Ma JX, Mao C et al. Nanoparticle-assisted targeted delivery of eye-specific genes to eyes significantly improves the vision of blind mice in vivo. Nano Letters. 2014; 14: 5257-5263.
7. Wong Y, Rajala A, Rajala RV. Lipid nanoparticles for ocular gene delivery. Journal of Functional Biomatererials, 2015; 6: 379-394.
8. Paterna JC, Moccetti T, Mura A, Feldon J, Bueler H. Influence of promoter and WHV post-transcriptional regulatory element on AAV-mediated transgene expression in the rat brain. Gene Therapy. 2000; 7: 1304-1311.
9. Donello JE, Loeb JE, Hope TJ. Woodchuck hepatitis virus contains a tripartite posttranscriptional regulatory element. Journal of Virology. 1998; 72: 5085-5092.
10. Wang Y, Macke JP, Merbs SL, Zack DJ, Klaunberg B, Bennett J et al. A locus control region adjacent to the human red and green visual pigment genes. Neuron. 1992; 9: 429-440.
11. Le YZ, Ash JD, Al Ubaidi MR, Chen Y, Ma JX, Anderson RE. Targeted expression of Cre recombinase to cone photoreceptors in transgenic mice. Molecular Vision. 2004; 10: 1011-1018.
12. Feng G, Mellor RH, Bernstein M, Keller-Peck C, Nguyen QT, Wallace M et al. Imaging neuronal subsets in transgenic mice expressing multiple spectral variants of GFP. Neuron. 2000; 28: 41-51.
13. Matsuda T, Cepko CL. Electroporation and RNA interference in the rodent retina in vivo and in vitro. Procedings of the National Academy of Sciences of the United States of America. 2004; 101: 16-22.
14. Shaner NC, Lambert GG, Chammas A, Ni Y, Cranfill PJ, Baird MA et al. A bright monomeric green fluorescent protein derived from Branchiostoma lanceolatum. Nature Methods. 2013; 10: 407-409.
15. Cao B, Xu H, Mao C. Transmission electron microscopy as a tool to image bioinorganic nanohybrids: the case of phage-gold nanocomposites. Microsccopy Research and Technique. 2011; 74: 627-635.
16. Punzo C, Cepko C. Cellular responses to photoreceptor death in the rd1 mouse model of retinal degeneration. Investigative Ophthalmology and Visual Science. 2007; 48: 849-857.
17. Tang PH, Buhusi MC, Ma JX, Crouch RK. RPE65 is present in human green/red cones and promotes photopigment regeneration in an in vitro cone cell model. Journal of Neuroscience. 2011; 31: 18618-18626.
18. Niwa H, Yamamura K, Miyazaki J. Efficient selection for high-expression transfectants with a novel eukaryotic vector. Gene 1991; 108: 193-199.
19. Miyazaki J, Takaki S, Araki K, Tashiro F, Tominaga A, Takatsu K et al. Expression vector system based on the chicken beta-actin promoter directs efficient production of interleukin-5. Gene 1989; 79: 269-277.
20. Buchholz CJ, Friedel T, Buning H. Surface-Engineered Viral Vectors for Selective and Cell Type-Specific Gene Delivery. Trends in Biotechnology. 2015; 33: 777-790.
21. Lai CM, Yu MJ, Brankov M, Barnett NL, Zhou X, Redmond TM et al. Recombinant adeno-associated virus type 2-mediated gene delivery into the Rpe65-/- knockout mouse eye results in limited rescue. Genetetic Vaccines and Therapy. 2004; 2: 3.
22. Bemelmans AP, Kostic C, Crippa SV, Hauswirth WW, Lem J, Munier FL et al. Lentiviral gene transfer of RPE65 rescues survival and function of cones in a mouse model of Leber congenital amaurosis. PLoS. Medicine. 2006; 3: e347.
23. Tan E, Wang Q, Quiambao AB, Xu X, Qtaishat NM, Peachey NS et al. The relationship between opsin overexpression and photoreceptor degeneration. Investigative Ophthalmology and Visual Science. 2001; 42: 589-600.
24. Xiong W, MacColl Garfinkel AE, Li Y, Benowitz LI, Cepko CL. NRF2 promotes neuronal survival in neurodegeneration and acute nerve damage. Journal of Clinical Investigations. 2015; 125: 1433-1445.
25. Futaki S, Suzuki T, Ohashi W, Yagami T, Tanaka S, Ueda K et al. Arginine-rich peptides. An abundant source of membrane-permeable peptides having potential as carriers for intracellular protein delivery. Journal of Biological Chemistry. 2001; 276: 5836-5840.
26. Schwarze SR, Ho A, Vocero-Akbani A, Dowdy SF. In vivo protein transduction: delivery of a biologically active protein into the mouse. Science. 1999; 285: 1569-1572.
27. Schwarze SR, Dowdy SF. In vivo protein transduction: intracellular delivery of biologically active proteins, compounds and DNA. Trends in Pharmacological Sciences. 2000; 21: 45-48.
28. Becker-Hapak M, McAllister SS, Dowdy SF. TAT-mediated protein transduction into mammalian cells. Methods. 2001; 24: 247-256.
29. Pepe S, Mentzer RM, Jr., Gottlieb RA. Cell-permeable protein therapy for complex I dysfunction. J Bioenergetic and Biomembranes. 2014; 46: 337-345.
30. Shin MJ, Kim DW, Lee YP, Ahn EH, Jo HS, Kim DS et al. Tat-glyoxalase protein inhibits against ischemic neuronal cell damage and ameliorates ischemic injury. Free Radical Biology and Medicine. 2014; 67: 195-210.
31. Harada H, Kizaka-Kondoh S, Hiraoka M. Antitumor protein therapy; application of the protein transduction domain to the development of a protein drug for cancer treatment. Breast Cancer. 2006; 13: 16-26.
32. Adler R, Curcio C, Hicks D, Price D, Wong F. Cell death in age-related macular degeneration. Molecular Vision. 1999; 5: 31.

33. Stone EM, Braun TA, Russell SR, Kuehn MH, Lotery AJ, Moore PA et al. Missense variations in the fibulin 5 gene and age-related macular degeneration. New England Journal of Medicine. 2004; 351: 346-353.
34. Bonilha VL. Age and disease-related structural changes in the retinal pigment epithelium. Clinical Ophthalmology. 2008; 2: 413-424.
35. Hollyfield JG, Bonilha VL, Rayborn ME, Yang X, Shadrach KG, Lu L et al. Oxidative damage-induced inflammation initiates age-related macular degeneration. Nature Medicine. 2008; 14: 194-198.
36. Berson EL. Retinitis pigmentosa: unfolding its mystery. Procedings of the National Academy of Sciences of the United States of America. 1996; 93: 4526-4528.
37. Punzo C, Xiong W, Cepko CL. Loss of daylight vision in retinal degeneration: are oxidative stress and metabolic dysregulation to blame? Journal of Biological Chemistry. 2012; 287: 1642-1648.
38. Gardner TW, Antonetti DA, Barber AJ, LaNoue KF, Levison SW. Diabetic retinopathy: more than meets the eye. Survey of Ophthalmology. 2002; 47 Suppl 2: S253-S262.
39. Cho NC, Poulsen GL, Ver Hoeve JN, Nork TM. Selective loss of S-cones in diabetic retinopathy. Archives of Ophthalmology. 2000; 118: 1393-1400.
40. Martin KR, Quigley HA. Gene therapy for optic nerve disease. Eye (Lond). 2004; 18: 1049-1055.
41. Caprioli J. Glaucoma: a disease of early cellular senescence. Investigative Ophthalmology and Visual Science. 2013; 54: ORSF60-ORSF67.